Biochimica et Biophysica Acta, 685 (1982) 51–60
Elsevier Biomedical Press

BBA 71042

ALAMETHICIN-INDUCED CHANGES IN LIPID BILAYER MORPHOLOGY

T.J. McINTOSH, H.P. TING-BEALL and G. ZAMPIGHI *

Department of Anatomy, Duke University Medical Center, Durham, NC 27710 (U.S.A.)

(Received July 14th, 1981)

Key words: Alamethicin; Lipid bilayer morphology; Freeze-fracture; X-ray diffraction

We have found that alamethicin, in the absence of an electric field, modifies both the hydrophilic surface and hydrophobic core of lipid bilayers. As shown by freeze-fracture and X-ray diffraction experiments with multiwalled vesicles, alamethicin increases the fluid space between bilayers by as much as 50 nm, and at the same time perturbs the hydrocarbon regions of the bilayers. For suspensions of gel-state lipid treated with alamethicin, uniformly spaced rows of particles cover the fracture faces and corresponding linear arrays of stain-collecting depressions cover the hydrophilic surfaces. In the liquid-crystalline state, alamethicin induces an irregular granular texture on the fracture faces.

Introduction

The polypeptide antibiotic alamethicin has been shown to induce voltage-dependent conductance in black lipid membranes. Molecular models [1–4], based on electrophysiological studies [1–8], have been proposed for the formation of the alamethicin conducting channels. It has generally been postulated that, in the absence of an applied electrical field, alamethicin resides at the membrane surface and channel formation involves the voltage-dependent insertion of alamethicin molecules into the hydrocarbon region of bilayers. After removal of the electric field, alamethicin molecules are thought to return to the membrane surface. These molecular models differ on whether the voltage-dependent insertion involves preformed oligomers [1,2] of alamethicin molecules or monomers [3] which diffuse laterally in the bilayer to form oligomeric conducting channels. For high aqueous concentrations of alamethicin, Eisenberg et al. [6] have observed voltage dependent conductance in planar bilayers in the absence of an applied field.

The interaction of alamethicin and phospholipids has also been studied by a number of physical techniques. Chapman et al. [9] found that alamethicin readily penetrated lipid monolayers and that increasing amounts of alamethicin decreased the intensity of the lamellar X-ray diffraction orders obtained from multiwalled lipid vesicles. Hauser et al. [10] interpreted their NMR data to mean that each alamethicin molecule 'induces a transition of about 600 lipid molecules from the normal multilamellar state to some new form of aggregate', thus abolishing multilamellar structure. These authors stated that the changes caused by alamethicin were primarily due to hydrophobic interactions. However, in a subsequent NMR study, Lau and chan [11] concluded that alamethicin was surface active, interacting primarily with the polar lipid head groups.

Recently, two groups have challenged the idea that alamethicin is inserted into the bilayer by application of an electric field. Fringeli and

* Present address: Jerry Lewis Neuromuscular Research Center, UCLA School of Medicine, Los Angeles, CA 90024, U.S.A.

Abbreviations: PC, phosphatidylcholine; DPPC, dipalmitoylphosphatidylcholine.

0005-2736/82/0000–0000/$02.75

Fringeli [12] employed infrared attenuated total reflection spectroscopy to examine the interaction of alamethicin with dipalmitoylphosphatidylcholine (DPPC), below the lipid thermal phase transition. Their data indicate that, under these conditions, in the absence of an electric field, alamethicin spans the lipid bilayer. Furthermore, using an analog consisting of an alamethicin molecule covalently bound to a phospholipid molecule, Latorre and Quay [13] were able to demonstrate voltage-dependent conductance similar to that of natural alamethicin. They interpreted these results to mean that alamethicin gating does not involve the insertion of alamethicin monomers into the membrane, but rather conformational changes of molecules already in the bilayers.

Our present study was undertaken to determine the effects of alamethicin on the morphology of lipid bilayers in the absence of an electric field. We wanted to determine, if, in fact, alamethicin alters the lipid bilayer hydrocarbon region, either above or below the lipid phase transition temperature. We were also interested in morphologically characterizing the lipid/alamethicin aggregates studied by Hauser et al. [10] and Chapman et al. [9].

Materials and Methods

Dipalmitoylphosphatidylcholine (DPPC), dimyristoylphosphatidylcholine (DMPC), and dilauroylphosphatidylcholine (DLPC) were used as obtained from Calbiochem (La Jolla, CA). Cholesterol was obtained from Supelco (Bellefonte, PA) while alamethicin was the kind gift of Dr. Joseph E. Grady, Upjohn Company, Kalamazoo, MI. During the final stages of this work, Dr. J.E. Hall of the Physiology Department of the University of California at Irvine also kindly supplied us with Upjohn alamethicin. Triple distilled water was used in all experiments.

Lipid and lipid/alamethicin suspensions were formed by the following procedures. For most experiments, the lipid/alamethicin specimens were dried from chloroform or ethanol solutions by use of a rotary evaporator. An appropriate amount of water (70% by weight relative to the lipid, unless otherwise stated) was added. Similar results were obtained when 0.1 M NaCl, adjusted to pH 7.4, was used instead of water. For certain experiments, as noted in the Results section, alamethicin was added through the aqueous phase. In these cases, a solution of 1 mg/ml alamethicin in water was added to the dry lipid. All mixtures were vortexed extensively and allowed to equilibrate at temperature above the lipid's phase transition temperature for several hours. The suspensions were then allowed to equilibrate at room temperature for at least one hour. All experiments were performed at 18°C ± 2°C.

For freeze-fracture experiments, small samples (0.1 μl) were sandwiched between two copper strips (giving a sample of 10 μm thickness and about 2.5 mm in diameter) and frozen in liquid propane at −190°C using the dropping device developed by Costello and Corless [14]. Frozen samples were loaded in a specially designed hinged device [15] under liquid N_2 and then transferred to the precooled stage of a Balzers BA-360 freeze-fracture instrument. The samples were fractured at −150°C and at about 10^{-7} Torr. Samples were immediately replicated with platinum-carbon from a 45° angle and carbon from a 90° angle. Replicas were cleaned in organic solvents such as chloroform/ethanol and picked up on uncoated 400 mesh electron microscope grids. All freeze-fracture micrographs are mounted so that the platinum deposition direction is from the bottom.

Negative staining was performed by depositing a diluted specimen on a freshly prepared carbon coated electron microscope grid. The grid was then washed with a solution of 1% uranyl acetate in water, blotted with filter paper, and allowed to dry at room temperature. All specimens were examined with a Philips 301 electron microscope operated at 80 kV with a 50 μm objective aperture.

For X-ray diffraction experiments, samples were sealed in quartz glass X-ray capillary tubes and mounted in an X-ray camera equipped either with a point-focus collimator or a mirror-monochromator system as described previously [16]. X-ray diffraction patterns were recorded on three or more layers of Kodak No-screen X-ray Film packed in a flat-plate film cassette. Specimen-to-film distances were between 6 and 10 cm and exposure times varied from 2 to 6 h. Densitometer traces were recorded on a Joyce-Loebl microdensitometer Model MK III C, the background

curve subtracted, and integrated intensities $I(h)$ were measured. Electron density profiles, $\rho(x)$ were calculated by use of the formula

$$\rho(x) \propto \sum_h \varphi(h) \sqrt{h^2 I(h)} \cos \frac{2\pi h x}{d}$$

where x is the distance normal to the lamellar repeat, d is the repeat period, and $\varphi(h)$ is the phase factor for each order h. $\varphi(h)$ must be + or − for these centrosymmetric systems. For control DPPC bilayers, the phase factors determined previously by Lesslauer et al. [17] were used. For DPPC/alamethicin suspensions, the phase factors were determined by assuming a bilayer-like profile for each lamellar unit. The freeze-fracture images, as well as the wide-angle and low-angle diffraction data (see Results) are diagnostic of bilayer phases [18]. For this relatively low-resolution data, only one phase combination produced an electron density profile which was consistent with a bilayer structure.

Results

The incorporation of alamethicin modifies both the hydrophobic and hydrophilic regions of the gel-state bilayer as determined by freeze-fracture and negative stain experiments, respectively. Fig. 1 shows a comparison of freeze-fracture replicas of DPPC in water (Fig. 1A) and of DPPC/alamethicin (0.05 mole fraction alamethicin) in water (Fig. 1B). In the control experiment, the DPPC bilayers are smooth and several fracture steps of uniform width can be seen. The specimen with alamethicin (Fig. 1B) also shows fracture steps of relatively uniform width. However, the fracture planes are no longer smooth, but display a series of rows or striations. On close inspection, it can be observed that many of these rows are actually lines of closely spaced particles. The spacing between adjacent rows is usually 6.0 to 7.0 nm, with the spacing between particles in each row more variable, about 5.0 to 7.0 nm. In certain areas, some rows stand out as ridges above adjacent rows (arrows in inset). Often alternate rows stand out as ridges so that the spacing between these prominent ridges (arrows in inset) is about 12 to 14 nm. The smooth ice between multilamellar regions is marked with an asterisk (*). Fig. 2 shows a DPPC/alamethicin specimen with a higher concentration of alamethicin (0.09 mole fraction) where adjacent rows are identical, with a fairly uniform spacing of about 6.0 nm between rows. In this image, there is a mosaic pattern to the specimen as it is composed of several areas with the rows in different orientations in adjacent patches. The arrowhead points to a boundary between two such regions. Occasionally, especially in areas of high curvature (arrow) the linearity is lost and one can observe a random arrangement of particles 6 nm in diameter, similar to the intramembrane particles found in biological membranes. In smaller lipid-peptide complexes (inset), particles are more difficult to distinguish and rows of particles are rarely observed.

Fig. 3 shows the appearance of a DPPC/alamethicin suspension by negative staining. In Fig. 3A a large structure, composed of several layers, is observed in the center of the field. The surfaces of this structure are covered with a lattice. Edge on views of the layers comprising the structure are marked by the arrow and show a lamellar arrangement, with the distance between lamellae being about 7.5 nm. Smaller structures, perhaps vesicles, are seen in the lower left corner of the field. Because many of these structures are multiwalled, the negative stain image is complicated by a superposition of many layers. Fig. 3B shows a field from the same preparation where it appears that single layers are visible (circles). In these regions, there are solid rows of stain alternating with rows where the stain has accumulated in an array of spots. The separation of the solid rows of stain is approx. 13 nm, with the linear arrays of spots centered between these rows. The distance between individual spots is somewhat variable, but usually about 6.5 to 7.5 nm. We have observed these linear arrays in DPPC suspensions with mole fractions of alamethicin between 0.02 and 0.20. The punctate nature of the arrays becomes more pronounced as the mole fraction of alamethicin is increased.

Some of the DPPC-alamethicin complexes which are smaller in size are shown in Fig. 4A and several important details should be noticed. First, many of these structures do not have the smooth edges characteristic of negatively stained vesicles

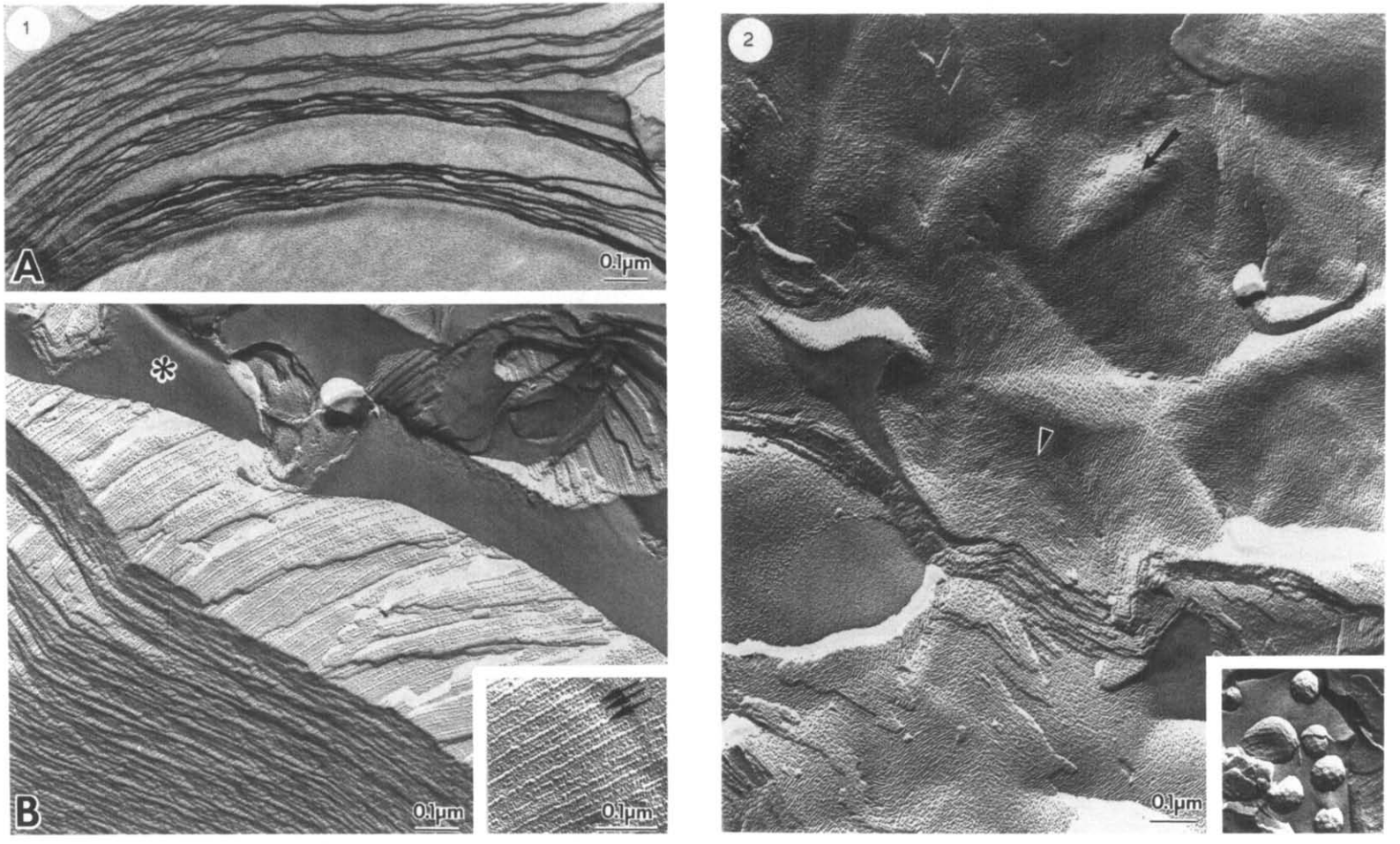

Fig. 1. Freeze-fracture images of (A) DPPC and (B) DPPC/alamethicin (0.05 mole fraction alamethicin) suspensions in 70% water at 18°C. Several fracture steps are seen in both replicas and the smooth ice between multilayer regions is marked by an asterick (*) in (B). The fracture faces are smooth in (A), but contain rows of particles in (B). In the inset, arrows point to alternate rows of particles which stand out as ridges above adjacent rows.

Fig. 2. Freeze-fracture image of a DPPC/alamethicin (0.09 mole fraction alamethicin) suspension. The fracture faces contain uniformly spaced rows of particles. The arrowhead points to a boundary between adjacent mosaic regions. The arrow indicates a region of randomly arranged particles. The inset, which was printed at approximately the same magnification as the main figure, shows the appearance of small lipid-peptide complexes.

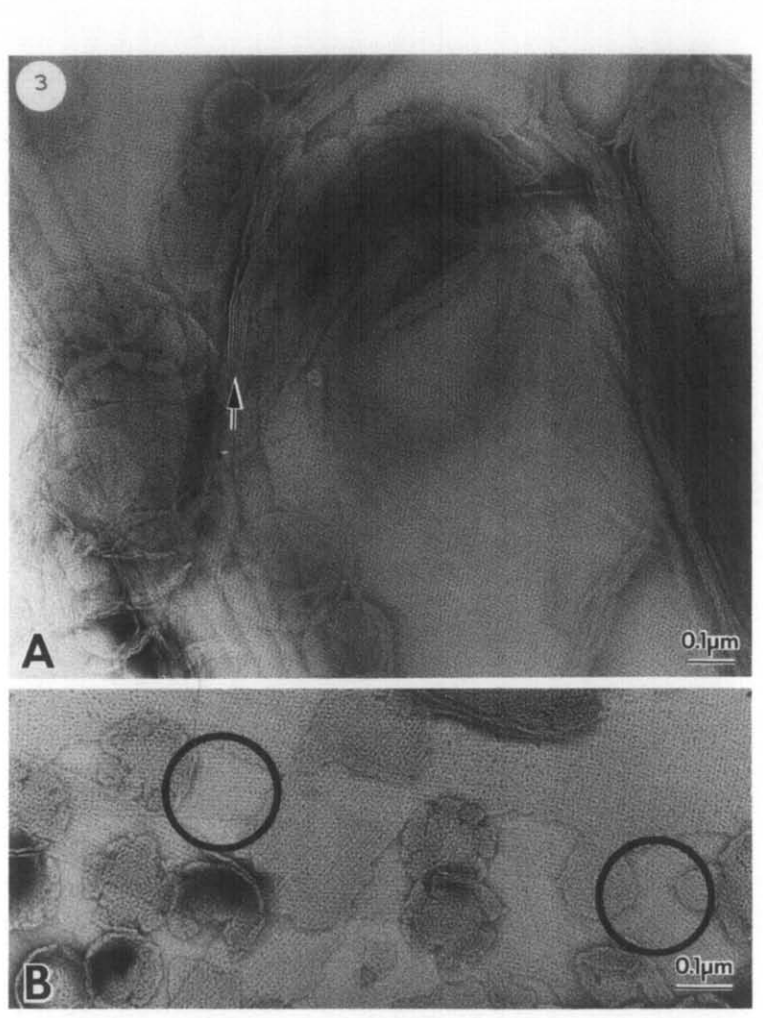

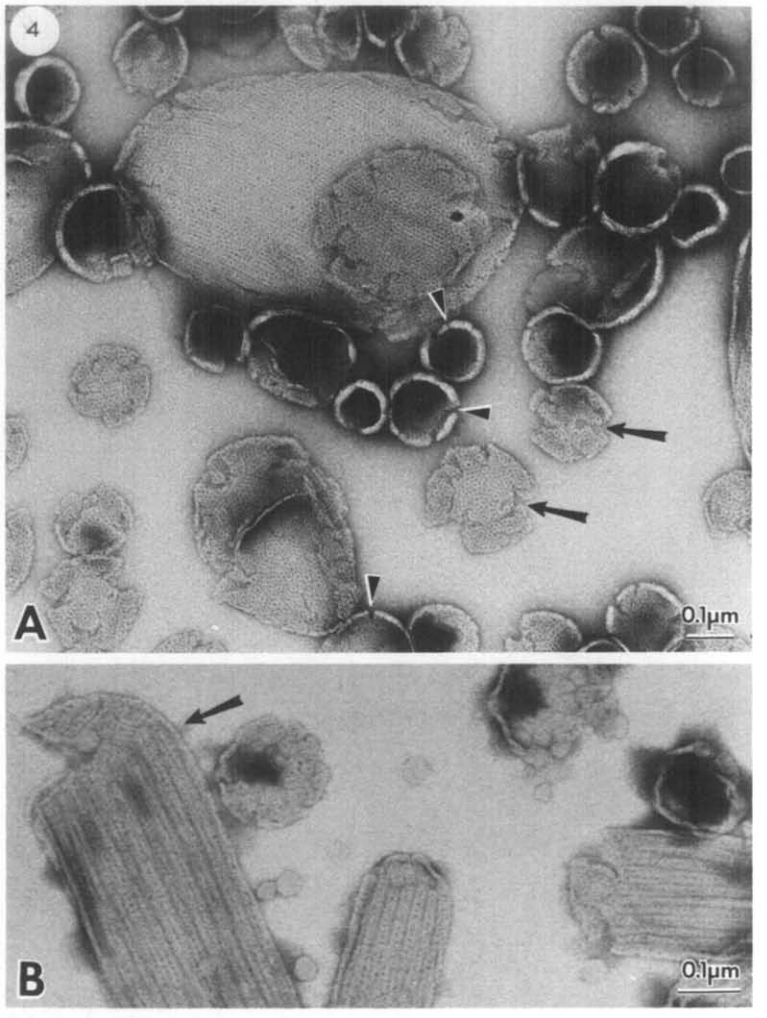

Fig. 3. Images of negatively stained DPPC/alamethicin (0.05 mole fraction alamethicin) suspensions. A large multilamellar region is shown in (A), and the regular array of stain observed in the plane of the bilayer arises from the superposition of patterns from several bilayers. The arrow points to a region where several layers are seen edge-on. In (B), there are areas (circles) where the staining pattern from a single bilayer can be observed. In these regions, solid rows of stain alternate with rows where the stain has accumulated in discrete spots.

Fig. 4. Images of negatively stained DPPC/alamethicin (0.05 mole fraction alamethicin) suspensions. In (A) arrows point to gaps or indentations at the edge of small lipid peptide aggregates, and the arrowheads mark these indentations seen in side-view. (B) is a higher-magnification view showing areas where the staining pattern is linear and smaller lipid/peptide aggregates where the staining pattern is less regular. The arrow points to a region where the two forms appear to merge.

[19,20]. Rather, there are gaps or indentations on the edges of these structures (arrows). Occasionally the sides of these structures curve upwards forming a cup where the stain accumulates. In these instances a side view can be seen. The arrowheads point to regions where the indentations at the edge of the structure can be seen in a side view. It appears that these are gaps or holes where stain can penetrate through the wall of the lipid. The smallest of these structures do not have linear arrays of stain, but appear to contain randomly arranged dots of stain. Thus, there are two appearances in the negatively stained DPPC/alamethicin suspensions: large, often multiwalled structures with linear arrays of stain and small, often single-walled structures, with randomly arranged dots of stain. Fig. 4B gives a higher magnification view of the DPPC/alamethicin aggregates. In the lower portion of the field is a region clearly displaying the alternating solid rows of stain and linear punctate arrays of stain. Near the top of the field are examples of the smaller lipid-peptide complexes. The arrow points to a region which shows a possible connection between these two forms of the DPPC-alamethicin complex. At the arrow the linear form is continuous with a piece of the more random form. It appears that the linear array breaks up as areas of lipid/peptide separate from the large structures.

Addition of alamethicin causes changes in both the wide-angle and low-angle X-ray diffraction patterns of gel state DPPC (see Fig. 5). The pattern from a suspension of gel state DPPC, as reported previously by others [18,21], consists of several orders of a lamellar repeat of 6.4 nm and a sharp wide-angle reflection at 0.42 nm, surrounded by a diffuse band (arrow). Suspensions of DPPC/alamethicin at the same water content relative to the lipid, show an increased lamellar repeat period of 7.8 nm ± 1.5 nm (average of four experiments) and a symmetric, but more diffuse, wide-angle reflection at 0.42 nm. There is also a very broad band centered at 0.85 nm which is not visible in Fig. 5B. The origin of this band is not known. Electron density profiles of multiwalled suspensions of DPPC and DPPC/alamethicin are shown in Fig. 6. In each profile, the two high density peaks represent the lipid head groups and the low density trough in the center corresponds to

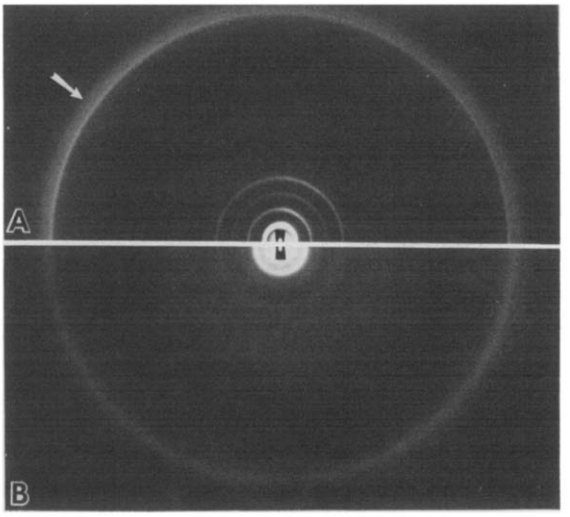

Fig. 5. Wide-angle X-ray diffraction patterns of (A) DPPC in 30%C water and (B) DPPC/alamethicin (0.17 mole fraction alamethicin) in 70% water. The wide-angle pattern from DPPC consists of a sharp ring at 0.42 nm surrounded by a diffuse band (arrow). This particular double reflection is also present in DPPC patterns with higher water contents [27]. For DPPC/alamethicin suspensions there is a single broad band in the wide-angle region centered at about 0.42 nm. Some low-angle lamellar reflections are visible in the center of the patterns.

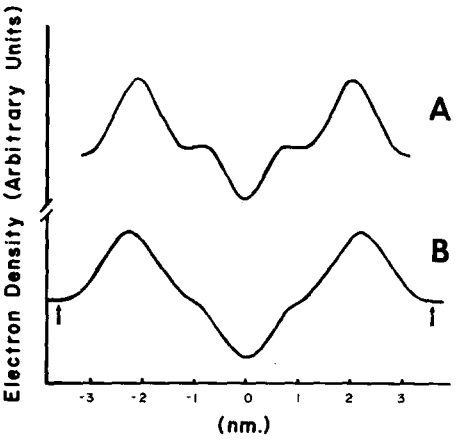

Fig. 6. Electron density profiles of (A) DPPC in 70% water and (B) DPPC/alamethicin (0.17 mole fraction alamethicin) in 70% water. The hydrophobic center of each bilayer is located at 0 on the abscissa. The width of each bilayer (as measured by high density head group peak separation) is greater for the DPPC/alamethicin suspension. The fluid layers between bilayers (marked by arrows) are also wider for the DPPC/alamethicin suspension.

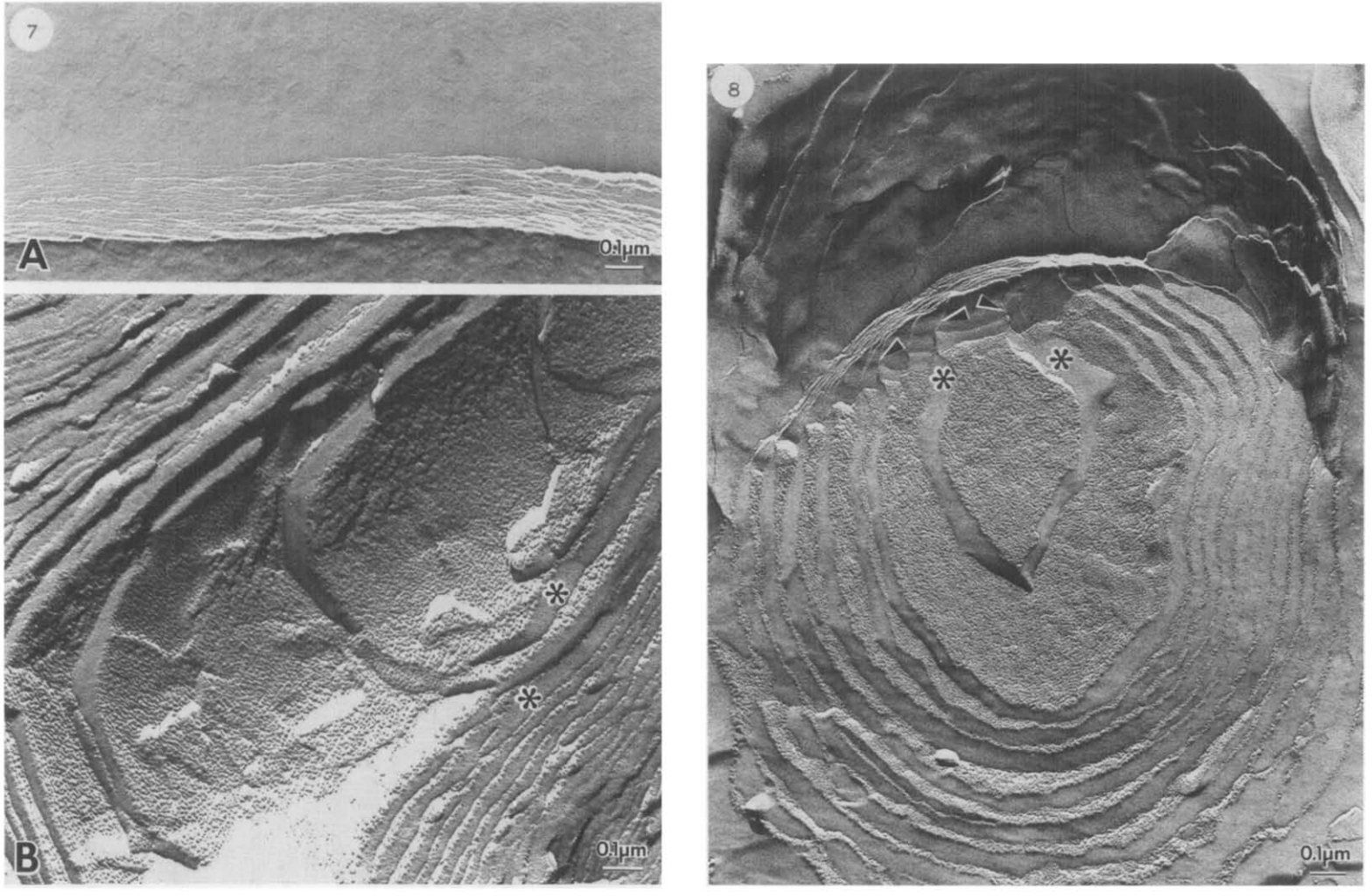

Fig. 7. Freeze-fracture images of suspensions of (A) DLPC and (B) DLPC/alamethicin (0.17 mole fraction alamethicin). The fracture faces of DLPC are smooth, while those from the DLPC/alamethicin suspension have a rough, grainy texture. Moreover, the fluid spaces between bilayers are much greater in the presence of alamethicin. Asterisks (*) denote two of the broad, smooth ice regions between adjacent hydrophobic fracture faces.

Fig. 8. Freeze-fracture image of a 2 : 1 : 0.25 molar ratio suspension of DMPC/cholesterol/alamethicin in 70% water. Arrowheads point to examples of fracture steps between smooth fracture faces, while asterisks mark wide ice layers between textured fracture faces. The continuity between rough and smooth fracture faces can be observed, indicating that alamethicin is segregated to certain regions in the plane of the bilayers.

the terminal methyl regions of the lipid hydrocarbon chains. In the DPPC profile, the medium density regions between the head group peak and terminal methyl trough correspond to the hydrocarbon methylene groups. This region is less distinct in the DPPC/alamethicin profile. The medium density regions at the outer edges of the profiles correspond to half of the fluid layers between bilayers. The fluid layers are approx. 1.1 nm wider when alamethicin is present (arrows).

Above the lipid phase transition, alamethicin modifies the morphology of the lipid bilayer, but in a manner different from below the transition. Fig. 7A shows a replica from a control experiment of a suspension of DLPC. Several clear fracture steps are seen, and the fracture faces are relatively smooth. In contrast, the fracture faces of a suspension of DLPC/alamethicin (Fig. 7B) are covered with an irregular grainy pattern. Moreover, the fracture steps are now much larger and considerable amounts of smooth ice (*) are seen between bilayers). The width between bilayers varies from 20 nm to 50 nm.

Fig. 8 shows a similar experiment with another liquid-crystalline lipid: a 2 : 1 mixture of DMPC/cholesterol. One large, multiwalled vesicle from a suspension of DMPC/cholesterol/alamethicin is shown. In this particular experiment, the mixing of the components was apparently not as complete as those shown in Fig. 7B, and this provides an unusual and revealing structure. At the top of the field, the hydrophobic surfaces of the vesicle are similar to the control bilayer (not shown) as the fractures faces are smooth and the fracture steps are quite narrow (arrow heads). However, near the bottom of the field, the hydrophobic surfaces are grainy and there are large ice spaces between the bilayers (*). Careful examination reveals that the smooth fracture faces at the top of this figure are continuous with the grainy fracture faces at the bottom. Moreover, the small, sharp fracture steps at the top are continuous with the broad fracture steps (occupied by smooth ice) at the bottom. In all areas the ice surrounding the vesicle is smooth. Similar results to those of Fig. 8 are obtained when aqueous solutions of alamethicin (1 mg/ml) are added to dry lipid. Again, two distinct fracture surfaces, smooth and grainy, are observed in the same sample. Invariably, small, sharp fracture steps are observed between smooth fracture faces, and broad fracture steps occur between grainy fracture faces.

Negative stain experiments showed no distinct differences in the hydrophilic surfaces of lipid and lipid/alamethicin suspensions for lipids in the liquid-crystalline state.

For lipid in the liquid-crystalline state, our X-ray diffraction results are similar to those of Chapman et al. [9]. The diffraction patterns from lipid/alamethicin suspensions contain broad bands instead of the sharp lamellar reflections obtained from large multiwalled vesicles. For the preparation shown in fig. 7B (a 5 : 1 molar ratio suspension of DLPC/alamethicin in excess water), the diffraction pattern consists of broad bands centered at approx. 3.0 nm, 0.85 nm, and 0.45 nm.

Discussion

The negative stain, freeze-fracture, and X-ray diffraction data show that, in the absence of an external electric field, alamethicin modifies both the hydrophilic and hydrophobic regions of gel state and liquid-crystalline state lipid bilayers. The evidence that alamethicin modifies the gel state bilayer's hydrophilic surface comes from negative stain images (Fig. 3 and 4) and low-angle X-ray diffraction patterns (Fig. 5) and electron density profiles (Fig. 6). Figs. 3 and 4 clearly show that alamethicin induces a linear and punctate negative staining pattern on the bilayer surface. The lamellar X-ray diffraction repeat period from alamethicin/DPPC suspensions is significantly larger than the repeat period from DPPC suspensions and the electron density profiles show that the fluid layers between bilayers are larger in the presence of alamethicin. Thus, at least part of the alamethicin molecule must reside at the bilayer surface to account for the punctate stain-filled depressions in the bilayer and the increased fluid width between bilayers. The increased fluid width is probably due to alamethicin increasing the repulsive force between the surfaces of adjacent bilayers. The freeze-fracture images shown in figs. 1 and 2, the wide-angle region of the X-ray diffraction patterns (Fig. 5), and the electron density profiles (Fig. 6), show that alamethicin perturbs the hydrophobic core of the bilayer.Freeze-fracture has been shown

to expose the geometric center of the bilayer [22,23]. In our images, alamethicin converts the normally smooth surfaces of DPPC (Fig. 1A) to rows of small punctate particles (Figs. 1B and 2). The change in shape of the X-ray reflection at 0.42 nm (Fig. 5) is direct evidence that alamethicin modifies hydrocarbon chain packing in the bilayer. The differences in the hydrocarbon regions in the profiles of Fig. 6 also indicate that alamethicin modifies this region of the bilayer. The bilayer width (head group-to-head group separation in the profile) is larger in the presence of alamethicin, probably due to a decrease in lipid hydrocarbon chain tilt [12].

For the case of liquid-crystalline lipids, the freeze-fracture images of Figs. 7 and 8 show that alamethicin modifies both the hydrophilic and hydrophobic regions of the lipid. The smooth hydrophobic faces of control bilayers are converted to grainy, rough surfaces by the incorporation of alamethicin and the fluid spaces between bilayers have swollen to 20 to 50 nm. The X-ray diffraction data also indicate that the fluid layers have increased with the incorporation of alamethicin. In control experiments, the DLPC suspensions give sharp lamellar reflections with a repeat period of 5.9 nm, which, based on swelling experiments with egg PC [24,25], is consistent with a fluid layer of about 1.5 to 2.5 nm. There are no sharp reflections for the DLPC/alamethicin suspension, and the broad band at about 3 nm is characteristic of the continuous transform of a single bilayer [17, 21, 26, 27]. The continuous transform is obtained when the fluid layers are very large and variable in thickness, as in a dispersion of membranes [26].

The differences in appearance of suspensions of gel state lipid alamethicin (Figs. 1–4) and liquid-crystalline state lipid alamethicin (Figs. 7, 8) can be explained in terms of the properties of the lipid matrix. DPPC has three distinct lamellar phases: the gel state ($L\beta'$ phase) at temperatures below the pretransition temperature of 35°C, the two-dimensional 'rippled' phase ($P\beta'$) between the pretransition and main transition, and the liquid-crystalline phase ($L\alpha$) above the main transition at 41°C [18,28]. Both the gel state and liquid-crystalline states have smooth fracture faces (Fig. 1A and Refs. 29, 30) and featureless surfaces by negative stain [19,20,31]. However, the $P\beta'$ phase has been shown to have a periodic ripple in the plane of the membrane at a spacing of between 12 and 15 nm [28]. This rippled phase can be observed as a series of striations in the hydrophobic surface by freeze-fracture [29–31] and in the hydrophilic surface by negative stain [31]. The linear regions of Fig. 4B resemble the rippled phase [31] except for the addition of the punctate dots of stain between the solid rows of stain. The freeze-fracture images (Fig. 2, in particular) resemble freeze-fracture images of the rippled phase except that often the distance between rows is half that of the $P\beta'$ phase and the rows have a punctate appearance. The 'mosaic' pattern of the rows in Fig. 2 is also very similar to the mosaic patterns seen in the $P\beta'$ phase [31]. It thus appears that alamethicin induces a phase similar to the $P\beta'$ phase (or, in effect, lowers the pretransition temperature) for DPPC multilayers. The broadening of the 0.42 nm X-ray relection is consistent with this interpretation [32]. It should be noted that there are other examples in the literature [33] where the introduction of an extraneous molecule into DPPC bilayers broadens the range of the $P\beta'$ phase. The alamethicin appears to interact with the bilayer at peaks and troughs of the rippled phase, areas of high curvature in the bilayer where the lipid hydrocarbon chain packing might be perturbed. In some manner, the alamethicin induces periodic punctate depressions along the peaks and troughs so that stain accumulates. However, as in negative stain images of the $P\beta'$ phase [31], more stain accumulates in the troughs than in the peaks and thus these troughs tend to be filled in with stain. This obscures the periodic punctate depressions in the troughs and produces the images seen in Figs. 3B and 4B of alternating solid and punctate rows of stain. In certain areas of Fig. 3B where the staining is very light, a punctate nature can also been seen in the usually solid rows of stain. The freeze-fracture process is also sensitive to the lipid alamethicin interaction and rows of small punctate particles are observed. Staining, of course, is not used in the freeze-fracture method so that there is no asymmetry in the peaks and troughs due to accumulation of stain. Thus, the distance between rows of particles in freeze-fracture experiments is often one-half of the distance between solid rows of stain in negative stain images. Occa-

sionally in the freeze-fracture replicas alternate rows of particles are elevated (see arrows, Fig. 1B). This is also evidently due to the peak and trough nature of the rippled phase. In the liquid-crystalline phase, there is no periodic lipid template, and alamethicin produces a random grainy pattern on the hydrophobic surface (Figs. 7B and 8). In certain specimens, particularly when cholesterol is present, the grainy pattern is located in patches in the plane of the bilayer (Fig. 8). This effect could be enhanced by the presence of cholesterol, as Cherry et al. [34] have noted that cholesterol induces a lateral segregation of proteins in the case of bacteriorhodopsin/phospholipid vesicles.

It is difficult to relate unequivocally these morphological results with electrophysiological data. Our experiments were performed using multiwalled vesicles with a higher content of alamethicin than is generally incorporated into planar black lipid membranes. Moreover, we were constrained to examine the lipid-alamethicin complexes in the absence of an applied electric field. However, it is significant that Eisenberg et al. [6] found conductance increases in the absence of an applied field when using high concentrations (10 μg/ml) of alamethicin in the aqueous phase. Thus, the images of Figs. 7 and 8 may represent morphological changes associated with alamethicin-induced voltage increases.

In conclusion, our data clearly show that alamethicin, even in the absence of an electric field, can substantially modify the hydrophobic core of vesicular bilayers. The 'new form' of lipid-peptide aggregates inferred by Chapman et al. [9] and Hauser et al. [10] appears to be a bilayer, but a highly modified bilayer.

Acknowledgements

We gratefully acknowledge many very useful discussions with Dr. M.J. Costello on the interpretation of freeze-fracture images. We appreciate the helpful suggestions of Dr. Ernest Helmreich, concerning the effects of cholesterol on lipid-peptide interactions, and of Dr. J.E. Hall, concerning alamethicin conductance. We thank Ms. Susan Gurganus and Ms. Pat Thompson for typing this manuscript. This work was supported by NIH grant R01 GM27278 (to T.J.M.).

References

1 Hall, J.E. (1975) Biophys. J. 15, 934–939
2 Boheim, G. and Kolb, H.-A. (1978) J. Membrane Biol. 38, 99–150
3 Baumann, G. and Mueller, P. (1974) J. Supramol. Struct. 2, 538–557
4 Smejtek, P. (1974) Chem. Phys. Lipids 13, 141–154
5 Mueller, P. and Rudin, D.O. (1968) Nature 217, 398–404
6 Eisenberg, M., Hall, J.E. and Mead, C.A. (1973) J. Membrane Biol. 14, 143–176
7 Gordon, L.G.M. and Haydon, D.A. (1976) Biochim. Biophys. Acta 436, 541–556
8 Fleischmann, M., Garielli, C., Labram, M.T.G., McMullen, A.I. and Wilmshurst, T.H. (1980) J. Membrane Biol. 55, 9–27
9 Chapman, D., Cherry, R.J., Finer, E.G., Hauser, H., Phillips, M.C. and Shipley, G.G. (1969) Nature 224, 692–694
10 Hauser, H., Finer, E.G. and Chapman, D. (1970) J. Mol. Biol. 53, 419–433
11 Lau, A.L.Y. and Chan, S.I. (1974) Biochemistry 13, 4942–4948
12 Fringeli, U.P. and Fringeli, M. (1979) Proc. Natl. Acad. Sci. USA 76, 3852–3856
13 Latorre, R. and Quary, S. (1981) Biophys. J. 33, 64a
14 Costello, M.J. and Corless, J.M. (1978) J. Microsc. 112, 17–37
15Costello, M.J. (1980) Scanning Electron Microsc. 2, 361–370
16 McIntosh, T.J., Simon, S.A. and MacDonald, R.C. (1980) Biochim. Biophys. Acta 597, 445–463
17 Lesslauer, W., Cain, J.E. and Blasie, J.K. (1972) Proc. Natl. Acad. Sci. USA 69, 1499–1503
18 Tardieu, A., Luzzati, V. and Reman, F.C. (1973) J. Mol. Biol. 75, 711–733
19 Bangham, A.D. and Horne, R.W. (1964) J. Mol. Biol. 8 660–668
20 Ting-Beall, H.P. (1980) J. Microsc. 118, 221–227
21 Torbet, J. and Wilkins, M.H.F. (1976) J. Theor. Biol. 62, 447–458
22 Branton, D. (1966) Proc. Natl. Acad. Sci. USA 55, 1048–1056
23 Deamer, D.W. and Branton, D. (1967) Science 158, 655–657
24 Small, D.M. (1967) J. Lipid Res. 8, 551–557
25 LeNeveu, D.M., Rand, R.P., Parsegian, V.A. and Gingell, D. (1977) Biophys. J. 18, 209–230
26 Wilkins, M.H.F., Blaurock, A.E. and Engleman, D.M. (1971) Nature New Biol. 230, 72–76
27 McIntosh, T.J. (1978) Biochim. Biophys. Acta 513, 43–58
28 Janiak, M.J., Small, D.M. and Shipley, G.G. (1976) Biochemistry 15, 4575–4580
29 Costello, M.J. and Gulik-Krzywicki, T. (1976) Biochim. Biophys. Acta 455, 412–432
30 Luna, E.J. and McConnell, H.M. (1977) Biochim. Biophys. Acta 466, 381–392
31 McIntosh, T.J. and Costello, M.J. (1981) Biochim. Biophys. Acta 645, 318–326
32 Rand, R.P., Chapman, D., and Larsson, K. (1975) Biophys. J. 15, 1117–1124
33 Stewart, T.P., Hui, S.W., Portis, A.R. and Papahadjopoulos, D. (1979) Biochim. Biophys. Acta 556, 1–16
34 Cherry, R.J., Müller, U., Holenstein, C. and Heyn, M.P. (1980) Biochim. Biophys. Acta 596, 145–151